Intelligence 65 (2017) 35–47

Contents lists available at ScienceDirect

Intelligence

journal homepage: www.elsevier.com/locate/intell

Network connectivity correlates of variability in fluid intelligence performance

Emiliano Santarnecchi[a,b,*], Alexandra Emmendorfer[a], Sayedhedayatollah Tadayon[a], Simone Rossi[b], Alessandro Rossi[b], Alvaro Pascual-Leone[a,c], on behalf of Honeywell SHARP Team Authors[a,d,e,f]

[a] Berenson-Allen Center for Non-Invasive Brain Stimulation, Beth Israel Medical Center, Harvard Medical School, Boston, MA, USA
[b] Medicine, Surgery and Neuroscience Department, Siena School of Medicine, Siena, Italy
[c] Institut Universitari de Neurorehabilitacio Guttmann, Badalona, Barcelona, Spain
[d] Honeywell Labs, Honeywell Aerospace, Redmond, WA, USA
[e] Electrical and Computer Engineering Department, Northeastern University, Boston, MA, USA
[f] Department of Experimental Psychology, University of Oxford, Oxford, UK

ARTICLE INFO

Keywords:
Fluid intelligence
Default mode network
fMRI
Ale
Functional connectivity

ABSTRACT

Abstract reasoning requires a pattern of spatial and temporal coordination among regions across the entire brain. Recent evidence suggests a very high similarity between spontaneous and evoked brain activity in humans, implying that a fine characterization of brain dynamics recorded during resting-state might be informative for the understanding of evoked behavior. In a recent work, we listed and detailed the sets of regions showing robust co-activation during the solution of fluid intelligence (*gf*) tasks, decomposing such meta-analytic maps in stimulus- and reasoning stage-specific sub-maps. However, while anatomical overlap with well-known resting-state fMRI networks (RSNs) has been documented, we here propose a quantitative validation of such findings via functional connectivity analysis in a sample of healthy participants. Results highlight a striking degree of similarity between the connectivity profile of the *gf* network and that of the dorsal attention network, with additional overlap with the left and right fronto-parietal control networks. Interestingly, a strong negative correlation with structures of the default mode network (DMN) was also identified. Results of regression models built on two independent fMRI datasets confirmed the negative correlation between *gf* regions and medial prefrontal structures of the DMN as a significant predictor of individual *gf* scores. These might suggest a framework to interpret previously reported aging-related decline in both *gf* and the correlation between "task-positive" networks and DMN, possibly pointing to a common neurophysiological substrate.

1. Introduction

Fluid intelligence (*gf*) represents the ability to solve problems regardless of previously acquired knowledge (Cattell, 1963). This ability contributes to efficient encoding of new information and its manipulation, constituting a pivotal component of human cognition with strong predictive power over both educational and professional success (Deary, 2008). At the same time, *gf* also represents one of the most elusive cognitive constructs, where theoretical and psychometric definitions have challenged scientists for half a century. While its theoretical definition seems challenging, with theories suggesting both uni- and multi-factorial nature of *gf*, its neurobiological underpinnings are probably even less understood. Modern technologies in neuroscience allow researchers to investigate brain activity at different spatial and temporal scales, allowing for inference about what, where, when and how *gf* resides in the human brain. Studies have provided correlates at the structural level, showing *gf*-related variability in the shape and volume of gray and white matter structures (Colom et al., 2009, 2013). Hypotheses about metabolic correlates of *gf* have been proposed as well, with evidence of a counterintuitive decrease in brain activity in higher *gf* individuals; a concept now well-accepted in the framework of a brain efficiency theory of intelligence (Haier et al., 1988). Studies investigating electrical brain activity using electroencephalography (EEG) have shown correlations with activity in specific frequency bands (Thatcher, Palmero-Soler, North, & Biver, 2016), as well as the importance of the coupling between multiple brain oscillatory patterns (Anja Pahor & Jaušovec, 2014). Finally, works looking at both evoked and spontaneous brain activity using functional magnetic resonance

* Corresponding author at: Berenson-Allen Center for Non-Invasive Brain Stimulation, Beth Israel Medical Center, Harvard Medical School, Boston, MA, USA.
E-mail address: esantarn@bidmc.harvard.edu (E. Santarnecchi).

http://dx.doi.org/10.1016/j.intell.2017.10.002
Received 30 April 2017; Received in revised form 15 October 2017; Accepted 17 October 2017

imaging (fMRI) (Cole, Yarkoni, Repovs, Anticevic, & Braver, 2012; Ebisch et al., 2012; Geake & Hansen, 2005, 2010; Preusse, Meer, Deshpande, Krueger, & Wartenburger, 2011), (Hearne, Mattingley, & Cocchi, 2016), have shown the relevance of a network of regions belonging to a so-called "parieto-frontal" network. This network, mostly involving brain regions of the prefrontal and parietal lobes bilaterally (Colom et al., 2013) (Vakhtin, Ryman, Flores, & Jung, 2014), resembles the map supporting the *parieto-frontal integration theory* (P-FIT) of general intelligence by Jung and Haier (2007), advancing the field a step closer to understanding the brain functional correlates of *gf*.

Recently, a fine characterization of such networks has been also proposed via a quantitative meta-analysis, including different anatomo-functional maps representing *gf*-related processing at the cortical and subcortical levels. The maps also include sub-maps specifically showing average brain activations for different types of reasoning (e.g. verbal vs visuospatial), those crucially recruited where more challenging trials are faced, as well as those engaged in different processing stages (i.e. Rule inference and Rule application) (Santarnecchi, Emmendorfer, & Pascual-Leone, 2017). This might help define within- and between-network dynamics subtending *gf* abilities, as well as targets for cognitive training (Anguera & Gazzaley, 2015) and brain stimulation interventions (Filmer, Dux, & Mattingley, 2014; Santarnecchi et al., 2015).

However, while such an anatomo-functional atlas of evoked activity provides useful information for understanding the brain correlates of *gf*, recent studies have also shown links between individual variability in *gf* abilities and the spontaneous organization of brain activity, as the one measured within the framework of functional connectivity functional magnetic resonance imaging (fMRI) analysis (van den Heuvel & Hulshoff Pol, 2010). Looking at the brain's spontaneous patterns of metabolic activity might be informative about - and even predict - individual evoked activity during sensorimotor and cognitive tasks (Fox et al., 2005), (Allen et al., 2014; Finn et al., 2015; Shirer, Ryali, Rykhlevskaia, Menon, & Greicius, 2012). Such intrinsic activity is thought to reflect not only the past experiences of each individual brain as a complex system, but it also forms the functional foundation from those evoked patterns which the brain will generate for future goal-oriented behavior (Tavor et al., 2016). Differently from canonical task-fMRI paradigms, where the signal is derived by contrasting brain activity during active and passive states, this approach relies on endogenous brain oscillations recorded during spontaneous brain activity, giving rise to a complex pattern of temporally and spatially independent resting-state networks (RSN) (Biswal et al., 2010). Such intrinsic organization of spontaneous brain activity is captured within the framework of brain connectivity analysis (Achard & Bullmore, 2007). Individual functional connectivity profiles have been proven reliable over multiple sessions (Braun et al., 2012), (Choe et al., 2015), holding enough information to identify pathological conditions (e.g. multiple sclerosis (Bonavita et al., 2016), schizophrenia (Bassett et al., 2008) and Alzheimer (Agosta et al., 2012)) as well as brain correlates of several cognitive (Santarnecchi, Polizzotto, Rossi, & Rossi, 2014), (Santarnecchi, Rossi, & Rossi, 2015; Yuan et al., 2012) and psychological traits (Adelstein et al., 2011).

An overview of the role played by regions activated during different *gf* tasks with respect to existing RSNs is not available to date, with recent meta-analytic data suggesting a major contribution by regions of the attention, salience and fronto-parietal control networks (Santarnecchi et al., 2017). However, thiss evidence, based on anatomical overlay between group-level RSNs maps and meta-analytic *gf* maps (using the activation likelihood estimate – ALE method), does not provide a comparison of actual functional connectivity patterns in humans and must be validated using real fMRI data. These, among other questions, should be answered: (i) Does the network of brain regions activated during *gf* problem-solving also constitute a functional network of positively correlated nodes at rest? (ii) Does the functional profile of *gf* activation maps resemble those of specific RSNs? (iii) If yes, which RSNs show higher similarity? Finally, (iv) are the different meta-analysis maps generated for *gf* also different in terms of their respective functional connectivity patterns? To address these questions, we analyzed resting-state fMRI data from a dataset of healthy participants. We quantitatively compared the functional connectivity profile of the meta-analytic *gf* (ALE) networks and well-known RSNs using a similarity index, also looking at intra- and inter-network dynamics by means of canonical functional connectivity metrics and topographical measures related to modularity and centrality. We predicted *gf* regions to be positively correlated at rest, to show similarity with cognitive networks such as the fronto-parietal control network (FPCN) and the dorsal attention network (DAN), as well as a negative correlation with the default mode network (DMN).

Moreover, given the link between evoked and spontaneous fMRI activity (Tavor et al., 2016), we hypothesized that the spontaneous activity of regions belonging to the ALE task-fMRI *gf* network would explain variability in behavioral *gf* scores. Therefore, separate regression models based on two independent fMRI datasets collected at Harvard Medical School (Boston, MA, USA) and University of Siena School of Medicine (Siena, Italy) were built, predicting individual *gf* abilities on the basis of seed-based connectivity patterns of the *gf* network.

2. Methods

2.1. Connectivity profile of the gf-network

The characterization of the functional connectivity profile of regions of the *gf* network (as described in (Santarnecchi et al., 2017), was based on data from the freely available dataset INDI-NKI Rockland, including structural and functional MRI data of 207 healthy participants (age 8 to 82). From the NKI-Rockland database, a selection of subjects was made to ensure *(i)* an age range between 18 and 55 years old (to focus on healthy adult individuals), *(ii)* an equal number of males and females, given the evidence of interactions between biological sex and intellectual abilities (Haier, Jung, Yeo, Head, & Alkire, 2005), *(iii)* an equal distribution of age groups (i.e. participants per decade) and *(iv)* that all subjects were right-handed. The selection resulted in a final sample of 130 right-handed subjects (69 males), with mean age of 36 years (range 18–55, SD = 13). Each contributor's respective ethics committee approved submission of de-identified data to be implemented into the ICBM dataset in the 1000 Functional Connectomes Project. The institutional review boards of NYU Langone Medical Center and New Jersey Medical School approved the receipt and dissemination of the data (Song et al., 2012). Details about the MRI protocols and preprocessing procedures are included in the supplementary materials.

2.2. Meta-analytic gf maps and regions of interests

We included meta-analytic maps based on activation likelihood estimate (ALE) technique as published in (Santarnecchi et al., 2017) and available at (http://www.tmslab.org/SantaLab.php/). Information about anatomical localization of each cluster and their meaning is provided in the original report. Each map is available as a nifti (nii) volumetric file in MNI space; both network and single node level maps are provided. Specifically, the following maps were used: main fluid intelligence (*gf*); *gf* activation for verbal (v*gf*) and visuospatial (vs*gf*) stimuli; activation during more challenging trials (higher complexity, HC); fMRI activation while participants infer the organizational principle of a given trial (Rule inference phase, RI) as well as when the newly inferred rule is applied to novel stimuli (Rule application phase, RA).

For RSNs, binary spatial maps were used following the scheme by Shirer et al. (2012), thus defining 14 non-overlapping maps

corresponding to: dorsal and ventral default mode (vDMN, dDMN), right and left executive control (RECN, LECN), the dorsal and ventral attention (AN), anterior and posterior salience (AS, PS), basal ganglia (BG), language (LANG), high and primary visual (HVIS, PVIS), precuneus (PREC), auditory (AUD) and somatosensory (SM) networks (Shirer et al., 2012).

It should be noted that different approaches for extracting and labeling RSNs have been applied by different research groups over the last 15 years. For instance, we here consider the AS as a network including bilateral insula (mostly referring to its anterior part) and dorsal anterior cingulate cortex (dACC); according to the work by Dosenbach and colleagues, the same network, with the inclusion of two anterior frontal regions corresponding to Brodmann area 9/10, is known as the cingulo-opercular network. Both names refer to a network associated with several executive functions, such as rule maintenance (Bunge et al., 2005), error-related activity and performance monitoring (Botvinick, Cohen, & Carter, 2004; Botvinick, Nystrom, Fissell, Carter, & Cohen, 1999; Carter et al., 1998). The same applies to the LECN and RECN, indicating two lateralized networks resembling the fronto-parietal control network as originally described by the same group (Dosenbach et al., 2007; Dosenbach, Fair, Cohen, Schlaggar, & Petersen, 2008). Both definitions, with the additional distinction of a left and right component in Shirer et al. (2012), refer to a network involved in cognitive control, with a specific involvement in control initiation, flexibility and modulation of response to feedback. Similarly, the AN identified here reflects the ventral and dorsal attention network proposed by Corbetta et al., with no differentiation between a dorsal (including bilateral parietal lobe, frontal eye fields and, to a lesser degree, parieto-occipital regions) and a ventral part (i.e. more frontal, including regions of the inferior and middle frontal gyrus) (Corbetta, Patel, & Shulman, 2008). This network is involved in attention-related processing, playing a major role in both top-down endogenous control of attention (dAN) and stimulus-driven reorienting (vAN) (Corbetta et al., 2008). Given the very high degree of overlap for the definition and anatomical localization of AS, AN and L/RECN across research groups, we will refer to these labels assuming the same conclusions are applicable to the cingulo-opercular network, ventral and dorsal attention networks as well as FPCN, discussing relevant difference where needed. Finally, another classification has been proposed by Yeo et al. (2011), including multiple labeling solutions acknowledging the existence of 7 or up to 17 resting-state fMRI networks. The main difference with respect to the work by Shirer et al. (2012) concerns the labeling of a subset of prefrontal regions, classified as part of the FPCN by Yeo et al. (2011) instead of AN (Shirer et al., 2012; Yeo et al., 2011). A graphical representation of both solutions and their differences is available in (Santarnecchi et al., 2017).

2.3. Regions of interest and statistical analysis

The average BOLD time course during resting-state has been retrieved for each ROI, namely each single node belonging to the *gf*, HC, v*gf*, vs*gf*, RI and RA ALE maps. Spontaneous BOLD activity was extracted both at the network level (e.g. v*gf* map) and single node level (i.e. including each region composing v*gf* as a separate ROI). The first approach was used when comparing the connectivity profile of a specific *gf* map and those of RSNs; single node analysis was performed to look at connectivity patterns within the *gf* network as well as while characterizing modularity structure of *gf* and RSNs (see paragraph on modularity). Single node analysis included each node of any *gf* map ($n = 96$) and those of the 14 RSNs ($n = 90$) by Shirer et al. (2012). For each model, a general linear model (GLM) including years of education, gender, age and total brain volume was built. To control for family-wise error (FWE) caused by the mass-univariate testing between 14 RSNs and *gf* maps, the network-based statistics (NBS) approach by Zalesky (Zalesky et al., 2010) was applied. Differently from the connections-based FWE control for multiple comparisons, NBS identifies potential connected structures/networks composed by connections exceeding a set of chosen thresholds, focusing the analysis on robust, repetitive functional structures present across all subjects and thus discarding isolate, potentially spurious connectivities. Here we applied a two-sided $p < 0.05$ threshold for pairwise connections and a NBS threshold of $p < 0.05$ for F statistics (1000 permutations).

2.4. Similarity analysis

The spatial similarity of seed-based connectivity maps for *gf* and RSNs was calculated using a metric similar to the DICE index (Dice, 1945). The comparison of weighted, unthresholded connectivity maps at the single voxel level requires taking into account not only spatial similarity, but also similarity of connectivity sign. Therefore, a similarity index was obtained by computing the product of each voxel's value across two maps (e.g. voxel *j* in the *gf* and DAN maps), resulting in a map where positive values represent voxels with the same sign in both maps, while negative ones represent opposite signs (e.g. positive connectivity value in voxel *j* in *gf*, negative in DAN). The magnitude of the similarity index represents the similarity of connectivity strength in the two maps (e.g. voxel *j* in *gf = 0.5; j* in DAN = 0.7; similarity = 0.35).

2.5. Modularity analysis

The presence of anatomical overlap between RSN maps and *gf* activation patterns might suggest similarities in the functional profile of these regions, however whether such regions belong to the same network may not be a logical consequence when their spontaneous fMRI activity is considered. Therefore, the connectivity matrices showing significant connections between any node of the RSNs and *gf* maps were used to verify their degree of affinity with common functional modules. A modularity index was calculated (Expert, Evans, Blondel, & Lambiotte, 2011) to identify modules/communities in the weighted, undirected graph, using the following formula:

$$Q = \frac{1}{2m} \sum_{i\ j} \left[A_{i,j} - \frac{Ki,Kj}{2m} \right] \delta(c_i, c_j)$$

where A_{ij} represents the weight of the edge between i and j, $k_i = \Sigma_j A_{ij}$ is the sum of the weights of the edges attached to vertex *i*, c_i is the community to which vertex *i* is assigned, the δ-function $\delta(u, v)$ is 1 if $u = v$ and 0 otherwise and $m = \frac{1}{2} \Sigma_{ij} A_{ij}$. The modularity of a partition is a scalar value between −1 and 1, measuring the density of links inside communities/modules as compared to links between them. Given the predictive power of resting-state patterns over evoked activity (Tavor et al., 2016), results of the modularity assessment based on actual fMRI data should resemble those of the anatomical overlap analysis. Given the overlap between nodes of different *gf* maps, three separate models were tested, considering the interactions between RSNs nodes and (i) *gf* & HC, (ii) v*gf* & vs*gf*, (iii) RI & RA.

Moreover, we aimed to identify nodes of the *gf* network with high centrality, reflecting brain regions showing a significant number of connections (i.e. functional connectivities) with other network nodes (Bullmore & Sporns, 2012). By computing the weighted degree of each node, this could help identify a core set of regions which potentially act as hubs for intelligence processing.

2.6. fMRI-based prediction of individual gf scores

In order to test the predictive power of *gf*-related regions over behavioral *gf* performance, two independent fMRI datasets including resting-state fMRI and cognitive data were used to provide more robust estimate. Data collected as part of two initiatives respectively (i) looking at the possibility of enhancing *gf* via a combination of cognitive training and non-invasive brain stimulation (i.e. “Strengthening Human

Adaptive Reasoning and Problem Solving" - SHARP study funded by IARPA, collected at the Beth Israel Deaconess Medical Center, Harvard Medical School, Boston, MA, USA; "SHARP" dataset hereafter), and (ii) investigating a possible link between spontaneous fMRI connectivity, cognitive profile and response to brain stimulation (i.e. APOLLO study, collected at the University of Siena, Italy; "Siena" dataset hereafter). Both initiatives included the acquisition of resting-state fMRI data and cognitive scores focused on *gf* and executive functions. The SHARP dataset includes 84 healthy participants (mean age 29 years, range 21 to 49, SD = 12; mean education 15 years, range 11 to 23, SD = 3) with fMRI data and two *gf* measures, namely the Raven Advanced Progressive Matrices (RAPM) and the Sandia matrix (Matzen et al., 2010); the Siena dataset includes 130 healthy participants (mean age 25 years, range 19 to 32, SD = 7; mean education 16 years, range 14 to 23, SD = 3) with fMRI data and RAPM scores. In SHARP, the average RAPM score was 0.77 (SD = 0.14), while the Sandia was 0.64 (SD = 0.17); in Siena, average RAPM scores was 0.54 (SD = 0.15). To provide estimates of the correlation between connectivity and behavior as test-unspecific as possible, RAPM and Sandia scores were averaged in the SHARP dataset. A regression analysis was computed by including the BOLD time course of the *gf*-network and individual *gf* scores, in each dataset. Age, gender and education were included as covariates in both regression models. Statistics was calculated using a two-sided $p < 0.05$ (False Discovery Rate correction) for single voxels and $p < 0.05$ (Family-Wise Error correction) at the cluster level. Details about the fMRI protocols for the SHARP and Siena datasets, as well as preprocessing procedures are included as part of the supplementary materials.

3. Results

3.1. *gf* network connectivity at rest

Within-*gf* network connectivity. Analysis of functional connectivity patterns between nodes of the *gf* network revealed a positively correlated structure, suggesting that regions activated during abstract reasoning are also correlated during spontaneous brain activity (Fig. 1A–B). Analysis of nodal degree highlighted two major hubs within the network, located in the inferior frontal gyrus (BA6) [$F_{(1130)} = 6.246$, $p < 0.05$] and inferior parietal lobule (BA40) [$F_{(1130)} = 5.145$, $p < 0.05$] (Fig. 1B).

gf network and the rest of the brain. By using the entire *gf* network as a single region of interest, seed-to-voxel connectivity maps were computed (Fig. 1C), showing a pattern of positive connectivity between nodes of the *gf* network (mostly in fronto-parietal structures, temporo-occipital junction and fronto-opercular regions) (Fig. 1C, in red). Interestingly, a strong negative correlation with structures resembling the default mode network was also identified, with an emphasis on medial regions such as the posterior cingulate, precuneus, anterior cingulate and medial prefrontal cortices (Fig. 1C, in blue).

3.2. *gf* and resting-state functional networks

Fronto-parietal RSNs. Cortical and subcortical maps for multiple RSNs were computed, allowing a comparison with *gf* network connectivity profile. As visible in Fig. 2, the *gf* network shows high similarity with multiple RSNs composed by regions of the prefrontal and parietal lobes of the brain. Highest similarity seems present for the DAN, while an opposite connectivity pattern is present for the DMN. As suggested by quantitative anatomical overlap (Santarnecchi et al., 2017), prefrontal regions of the *gf* network also show similarity with the AS and left EC networks, suggesting more specific matching in the parietal lobes (with DAN) and more distributed overlap in the prefrontal lobe. The DICE similarity analysis (Fig. 3) confirmed the same pattern, with higher overlap between *gf* and DAN, LECN and RECN, followed by BG, AS and PS networks.

Primary sensory and language RSNs. As visible in Fig. 4, a there is a significantly lower similarity between the *gf* network and RSNs related to language, visual, auditory and sensorimotor processing. The same applies for RSNs involving activity of the basal ganglia and the posterior salience network.

Functional connectivity results. Figs. 2–4 visually highlight the similarity between the *gf* network and RSNs. A quantitative estimate of their overlap was done by means of functional connectivity (Fig. 5) and graph theoretical modularity (Fig. 6) analyses. A connectivity analysis assessing the interaction of each RSN and *gf* network highlighted a complex pattern of positive and negative interactions across RSNs ($p < 0.05$, FDR corrected at single node level and NBS corrected at network level), with the *gf* network showing a strong positive connectivity with the DAN. Interestingly, this connection seems to be the strongest among all the pairwise connections (Fig. 5A). By limiting the analysis to the *gf* network as the only seed region, analysis confirmed the high correlation with the DAN (Fig. 5B), with second best connections involving the AS and left/right EC network. As shown in Fig. 5B, positive and negative connectivities were grouped on the basis of a functional clustering algorithm, resulting in the aforementioned DAN/ECN cluster, as well as another – weakly – positively associated set of RSNs including the AS, PS and BG, and two negatively correlated ones (primary visual and dorsal DMN).

Modularity analysis. Modularity results are reported by colour-coding each node in the graph according to its affinity with a given module (Figs. 6, S1 and S2). As expected, the modularity assessment showed that *gf* nodes do not constitute separate communities but are integrated in modules also including RSN nodes. The modular structure resembled the small-world topology previously documented for the human brain (Eguiluz, Chialvo, Cecchi, Baliki, & Apkarian, 2005), and substantially confirmed the results of the anatomical overlap. Due to the thresholding procedure operated via NBS, graphs depicted in Fig. 6 only include RSNs and *gf* nodes connected via strong connections, both positive and negative in nature. The approximate network sparsity of each matrix in Figs. 6, S1 and S2 are, respectively, 15%, 17% and 13%. Nodes of *gf* show highest affinity with three modules including nodes of the AN, AS, L/RECN and BG networks (Fig. 6). Regions activated during higher difficulty trials show association with L/RECN, but also modules including BG, AUD, PS and SM nodes (Fig. 6). The vast majority of vg*f* and vs*gf* nodes belongs to a module including AN, vDMN, L/RECN, BG and precuneus nodes (Fig. S1); remaining nodes show affiliation with different modules composed by d/vDMN, PS and HVIS networks. Finally, RI and RA nodes reflect the pattern highlighted by anatomical overlap: RI shows almost an exclusive association with AN nodes, while RA nodes are included in modules with v/dDMN, LANG, PS, AS, BG and SM (Fig. S2).

3.3. Connectivity profile of *gf* sub-networks

The connectivity profile of different *gf* maps derived using the ALE meta-analysis framework is displayed in Fig. 7. The maps referred to brain activations for (i) different types of stimuli (verbal and visuo-spatial), (ii) different trial difficulties, as well as (iii) non-overlapping processing stages (Rule inference and Rule application), and reveal high similarity with the overall *gf* network, except for the Rule application network which displays strong connectivity within the primary visual network and a negligible recruitment of fronto-parietal structures. Interestingly, processing based on visuo-spatial stimuli showed stronger positive connectivity with bilateral frontal eye fields, compared to verbal *gf* connectivity. Finally, problem solving involving more

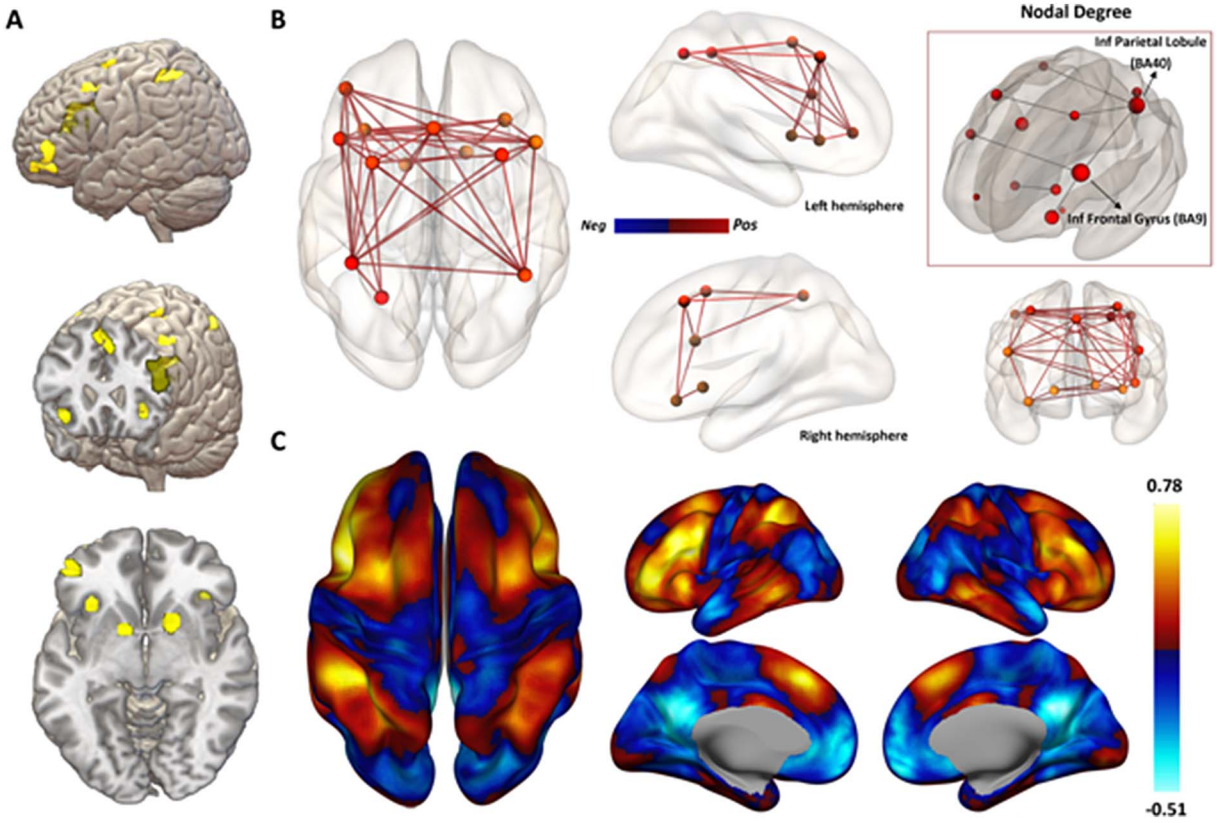

Fig. 1. Functional connectivity profile of *gf* network. Analysis was based on the original meta-analysis map representing the average fMRI activation published in (Santarnecchi et al., 2017) (A) Functional connectivity including all the nodes of the *gf* network highlighted a positively correlated network at rest (B) with highest centrality values for two regions in the frontal and parietal lobe of the brain (inset). (C) Seed-based connectivity using the entire *gf* network as a region of interest shows strong positive correlations among nodes of the network (yellow-red values) and a negative correlation with medial structures resembling the default mode network (DMN, blue values). (For interpretation of the references to colour in this figure legend, the reader is referred to the web version of this article.)

complex trials engages a network of bilateral fronto-parietal regions still resembling the DAN, but with a stronger involvement of regions in the right hemisphere, and stronger positive connectivity within the network overall.

3.4. Behavioral correlation

Results for the SHARP (A) and Siena (B) datasets are displayed in Fig. 8. The regression model identified similar patterns of negative correlations between spontaneous activity of the *gf* network and the inferior-medial prefrontal cortex in both datasets, as well as temporal pole and left angular gyrus in the Siena dataset. The two models yielded predictive power over *gf* scores by explaining ~23% and 14% variance in *gf* for, respectively, the SHARP and Siena data. The negative correlation suggests that individuals with stronger negative correlations between *gf* and the aforementioned regions score higher at behavioral *gf* assessment (see scatterplots in Fig. 8). The R^2 values were calculated by including the time series of the inferior-medial prefrontal lobe cluster overlapping in the SHARP and Siena datasets.

4. Discussion

In a recent investigation, we reviewed the literature about fMRI activation studies related to *gf* and derived meta-analytic spatial maps representing the anatomical localization of cognitive processes related to abstract reasoning (Santarnecchi et al., 2017). In the present study, we expanded such findings by investigating the relationship between functional connectivity patterns of *gf*-related maps and those of well-known resting-state fMRI networks. Moreover, we investigated the link between the connectivity profile of the *gf* network and individual *gf* scores in two independent datasets. The *gf* network showed positive correlations between its nodes at rest. Visual and quantitative analyses also revealed a major similarity with multiple fronto-parietal RSNs, with high overlap with the dorsal attention and left/right executive control networks. The strength of the negative correlation between *gf* regions and inferior-medial prefrontal regions of the default mode network also explained variability in *gf* scores in both datasets. We here discuss potential implications, including those related to target selection in cognitive enhancement studies based on non-invasive brain stimulation. For a discussion about hemispheric distribution of each *gf* map, the role of subcortical structures as well as of language-related and cerebellar regions, we refer to the discussion section in the original report.

4.1. Fluid intelligence and resting-state brain networks

Starting with the first neuroimaging evidence of *gf*-related activations using PET imaging (Haier et al., 1988), a major role for regions in the prefrontal and parietal lobes of the brain has been suggested and supported by extensive literature (Jung & Haier, 2007) (Colom et al., 2009). Given that prefrontal and parietal regions engage in wide cognitive functions, such a fronto-parietal-centric view of human intelligence seems a reasonable assumption. However, functional overlap between *gf* activation maps and RSNs show the involvement of multiple functional networks potentially responsible for different, non-overlapping components of *gf* processing. Most importantly, in the era of functional connectivity and network neuroscience, the localization of brain correlates of *gf* in the form of network-related dynamics has become crucial (Achard & Bullmore, 2007; Sporns, 2013). The present findings suggest a few interesting insights about the relationship

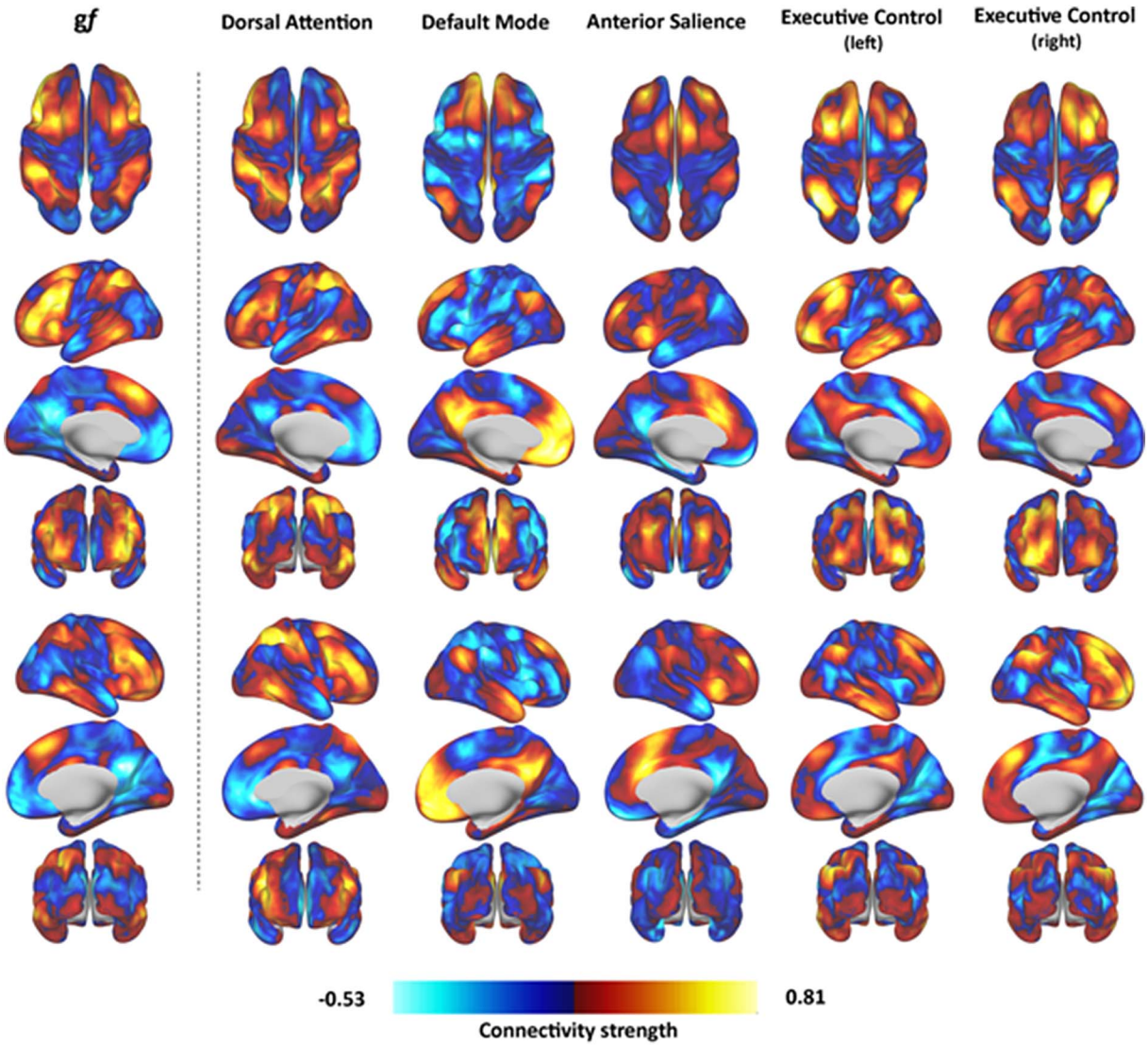

Fig. 2. *gf* and fronto-parietal resting state networks. A visual comparison of seed-based connectivity maps for *gf* network and major resting-state networks loading on prefrontal and parietal regions is shown. Red and blue colors represent the intensity and polarity of correlations between each network mask (top) and the rest of the brain. As clearly visible, the *gf* network shows very high similarity with connectivity profile of the dorsal attention network, especially for its parietal components. Overlap is also visible with activity in the anterior salience and left fronto-parietal control networks. Interestingly, *gf* regions show a negative correlation with activity in regions of the default mode network. (For interpretation of the references to color in this figure legend, the reader is referred to the online version of this chapter.)

between *gf* and brain connectivity. First of all, we confirmed that regions commonly co-activated during *gf* problem solving also show positive resting-state correlations, in agreement with recent evidence suggesting the high resemblance of evoked and spontaneous activity in the human brain (Tavor et al., 2016). Moreover, this also allowed the identification of regions of high connectivity within the *gf* network, suggesting regions in the left inferior frontal lobe and inferior parietal lobule as primary network hubs, and reinforcing the pivotal role for left fronto-parietal regions (Jung & Haier, 2007). Moreover, analysis of the connectivity between the *gf* network and the rest of the brain have confirmed the pattern previously observed via anatomical overlap analysis (Santarnecchi et al., 2017), suggesting a higher degree of similarity between *gf* regions and three fronto-parietal resting-state networks, namely the dorsal attention (as conceptualized by Corbetta and colleagues), and the left/right executive control networks (by Shirer et al., corresponding to the fronto-parietal control network in Dosenbach et al.).

The high resemblance between *gf* and DAN suggests a need for more specific labels than "fronto-parietal", which intuitively suggest the primary – or exclusive – involvement of regions involved in cognitive control, i.e. nodes of the left-right executive control networks. Looking at the specific role of the different DAN components and their relevance for *gf* processing, a separation within the attention network is needed. According to the original work by Corbetta et al. (2008), the attention network can be decomposed into a dorsal fronto-parietal module (or dorsal attention, resembling the DAN in the present work), which enables the selection of sensory stimuli based on internal goals or expectations (i.e. goal-driven attention) and links them to appropriate motor/cognitive responses; and a ventral fronto-parietal (or ventral attention) module, detecting salient and behaviorally relevant stimuli in the environment, especially when unattended (stimulus-driven attention). One implication might be that individual differences in *gf* are heavily related to the ability to focus on the task at hand while also suppressing distractors (both endogenous and exogenous), therefore maximizing cognitive capacity over relevant information. The competition model of attention proposes that objects in a visual scene compete for access to visual short-term memory and that the competition is biased by top-down signals that promote access of behaviorally relevant objects (Desimone & Duncan, 1995). These top-down signals interact with sensory (bottom-up) signals produced by objects in the visual

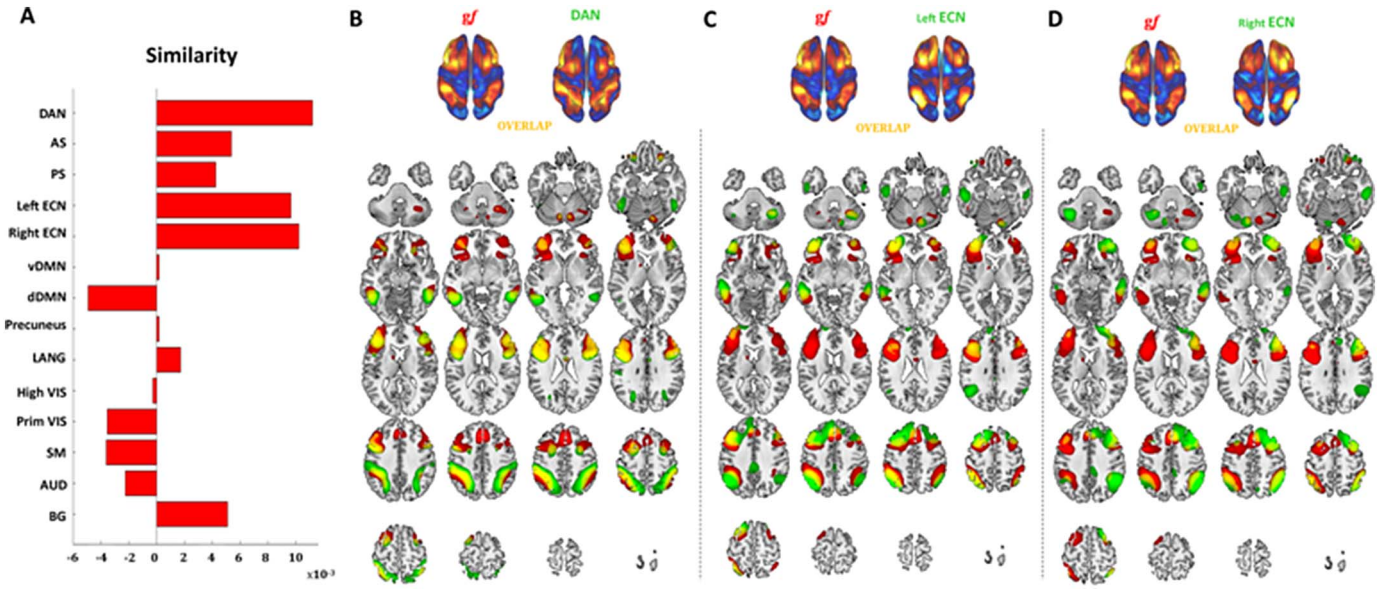

Fig. 3. Similarity coefficient. Coefficients for every RSN are shown (A), confirming the higher similarity between *gf* and DAN, left and right FPCN, as well as the dissimilarity with the DMN. Graphical overlap with DAN (B), left (C) and right FPCN (D) are also reported. Note: RSN = resting-state network; ventral and dorsal DMN (vDMN, dDMN); right and left executive control networks (right EC, left EC); dorsal attention network (DAN), anterior and posterior salience networks (AS, PS), basal ganglia network (BG); language network (LANG); high and primary visual networks (HighVIS, PrimVIS); precuneus network (Precuneus); auditory network (AUD); somatosensory network (SM).

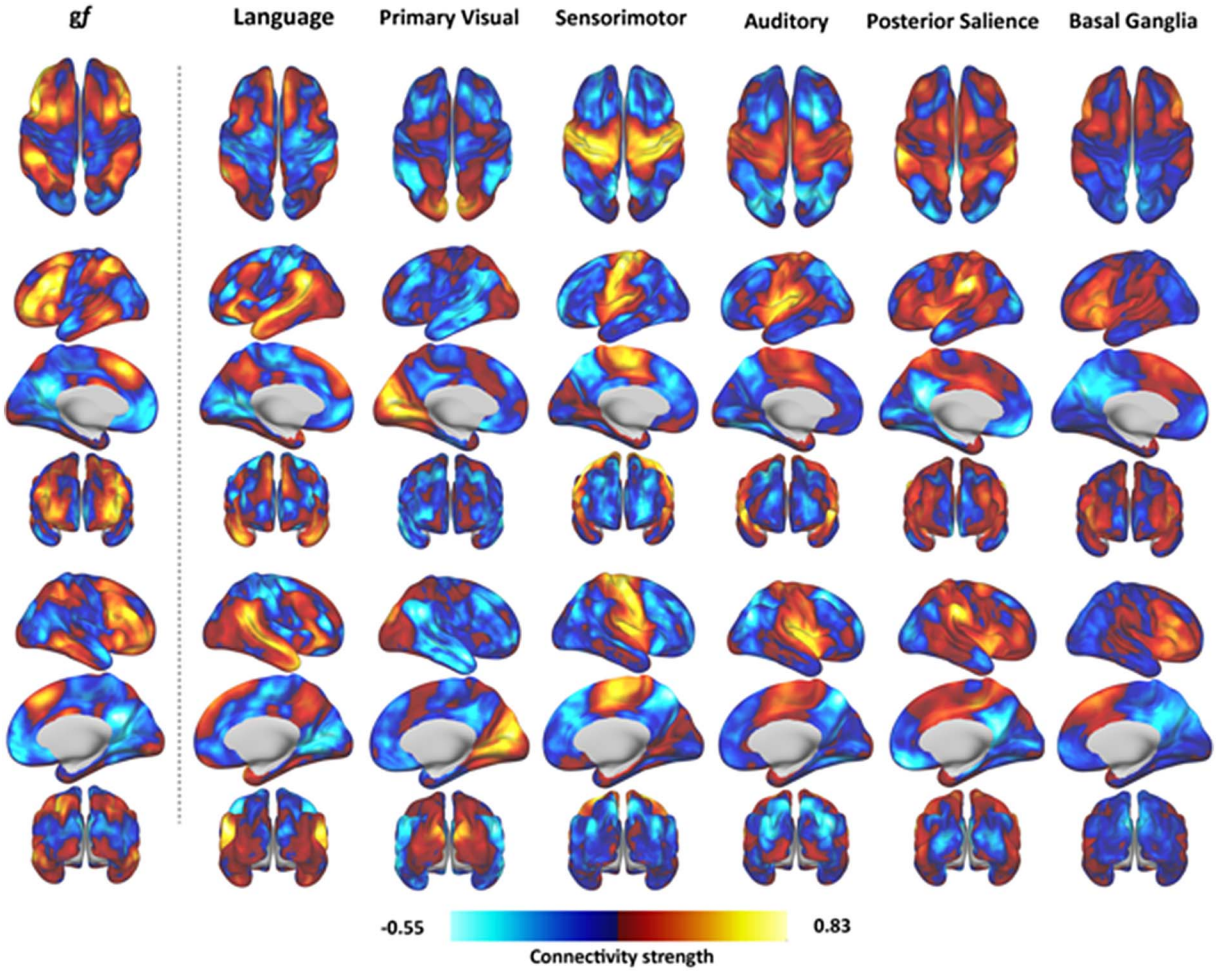

Fig. 4. *gf* and resting state network. The same visual comparison displayed in Fig. 2 is shown for networks related to sensory processing (visual, auditory and sensorimotor) as well as language, salience and subcortical activity related to the basal ganglia. In contrast to what was observed with the fronto-parietal resting-state networks, no significant overlap with *gf* activation sites seems to be present.

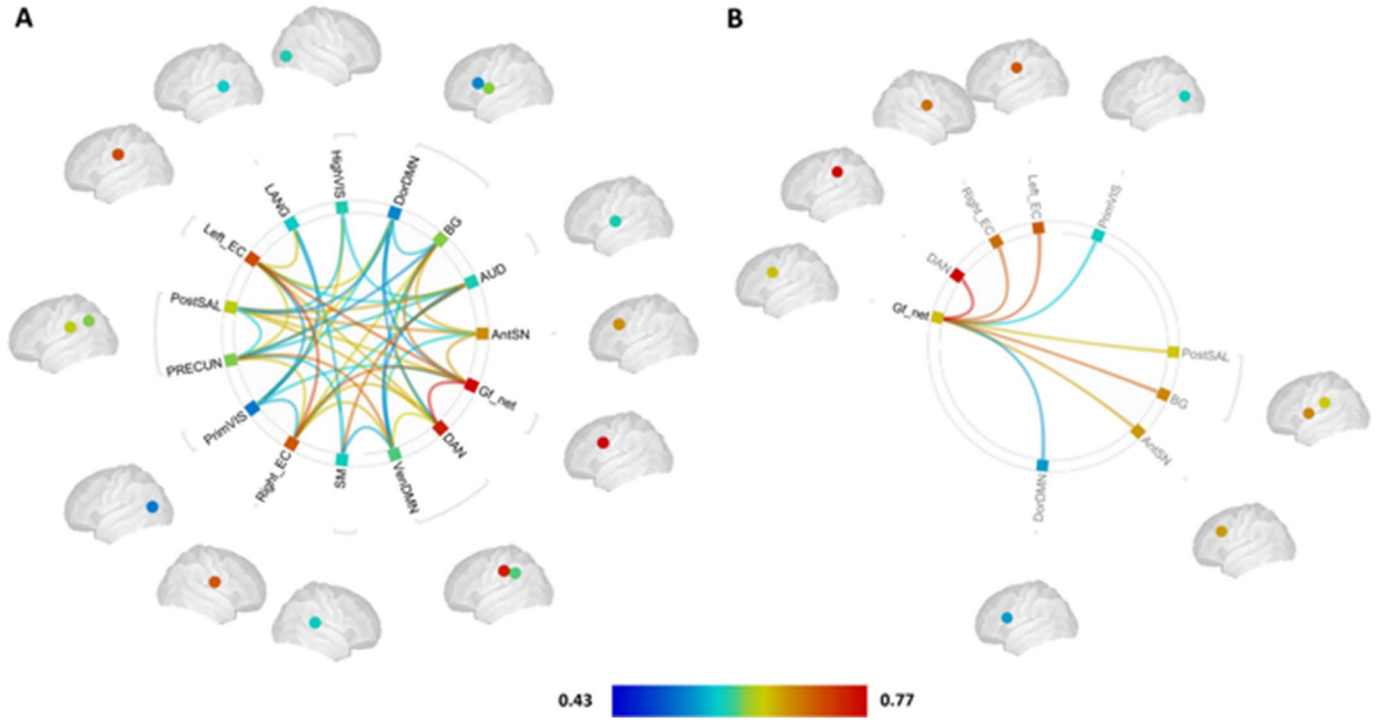

Fig. 5. Functional association at rest. The functional connectivity between *gf* network and other RSNs is shown, with positive and negative edges representing positive and negative connectivity at rest. As expected, *gf* network (*gf*_net) displays strong positive correlation with the DAN, whose correlation also represents the strongest (positive) one (A). Analysis focusing on *gf* network and its connections is shown in (B), displaying a hierarchy of similarity with the DAN, right and left fronto-parietal control networks as the most positively connected networks, followed by posterior salience, basal ganglia and anterior salience. Negative correlations are also present, as shown in Figs. 2 and 3, with only significant results involving the dorsal DMN and primary visual network ($p < 0.05$ FDR). Note: RSN = resting-state network; ventral and dorsal DMN (venDMN, dorDMN); right and left executive control networks (right EC, left EC); dorsal attention network (DAN), anterior and posterior salience networks (AntSN, PosSN), basal ganglia network (BG); language network (LANG); high and primary visual networks (HighVIS, PrimVIS); precuneus network (PRECUN); auditory network (AUD); somatosensory network (SM).

scene, enabling the target object to be selectively perceived/encoded and thus get access to memory storage at the expense of unimportant objects (Bundesen, 1990). Reducing the amount of information actively maintained in working memory could create cascade effects over higher order processes related to *gf*, freeing up computational space for hypothesis testing and validation. Testing more hypotheses might consequently have dramatic impact for cognitive abilities tested using time-constrained assessment. For instance, evidence of increased BOLD-fMRI activity in the visual cortex of subjects with high-functioning autism has been documented as the only significant correlates of their above-average *gf* abilities (Soulieres et al. 2009), with increasing trial complexity translating in reallocation of resources towards occipito-temporal regions (Simard, Luck, Mottron, Zeffiro, & Soulieres, 2015). One hypothesis might be that higher *gf* abilities are more related to optimization of low-level cognitive processes (visual, auditory, somatomotor) and their top-down control by attentional systems, than pure computational power needed for hypothesis testing and validation. At a more theoretical level, this does not mean individual *gf* abilities are more tightly associated with attention per se, with behavioral evidence addressing the interplay between *gf*, attention and executive functions actually showing moderate associations between the three domains (for a review see (Colom, Chuderski, & Santarnecchi, 2016)). The specific role regions of the DAN might play in *gf* processing can only be validated experimentally, with combined resting-state/activation fMRI studies.

As for the executive control network (FPCN in Dosenbach et al.), its role in controlling attention allocation and providing flexibility by adjusting response to feedback might be the key to its contribution to *gf* processing. Complementary to the cingulo-opercular/anterior salience network, the ECN is responsible for task engagement and, most importantly, for the online monitoring of cognitive (mostly attentive) resources. Data have shown how regions of the lateral frontal cortex overlapping with the left/right ECN are active when a cue is evaluated but attention is not shifted (Woldorff et al., 2004), promoting the idea of the prefrontal component of the ECN supporting some sort of shielding against “distractors”, which might represent a fundamental ability during *gf* problem solving.

The link with activity within the anterior and posterior salience networks might be explained by their role in the stable maintenance of task and rule mode (Bunge et al., 2005), as well as performance monitoring (M. M. Botvinick, Braver, Barch, Carter, & Cohen, 2001; M. M. Botvinick et al., 2004; Carter et al., 1998). In fact, a recent study has proposed a major role for the salience network in explaining variability in intelligence (Yuan et al., 2012), whereas the relevance of anterior salience's nodes, i.e. dACC and anterior insula, have been extensively associated with cognitive control and error detection in humans given their involvement in top–down control over sensory (Crottaz-Herbette & Menon, 2006) and limbic brain regions (Etkin, Egner, Peraza, Kandel, & Hirsch, 2006). Interestingly, while these functions might be relevant for the solution of a *gf* task, the link between these regions and arousal-related processes has been also considered (Braver & Barch, 2006). Dosenbach and colleagues have shown these regions being mostly associated with task-initiation cues and error cues, a potential proof of their role in both control/monitoring and arousal (given the relevance of the cues) which is then also maintained at an above-baseline level throughout the task (Dosenbach et al., 2008, 2006).

In the original ALE map (Santarnecchi et al., 2017), increasing complexity in *gf* trials corresponds to increased activity in a network of regions including the left inferior frontal lobe, left frontal eye fields, bilateral anterior cingulate cortex and bilateral temporo-occipital junction fMRI analysis shows positive connectivity in a bilateral fronto-parietal network, with stronger local connectivity in the right prefrontal lobe as compared to the main *gf* network. This information might be

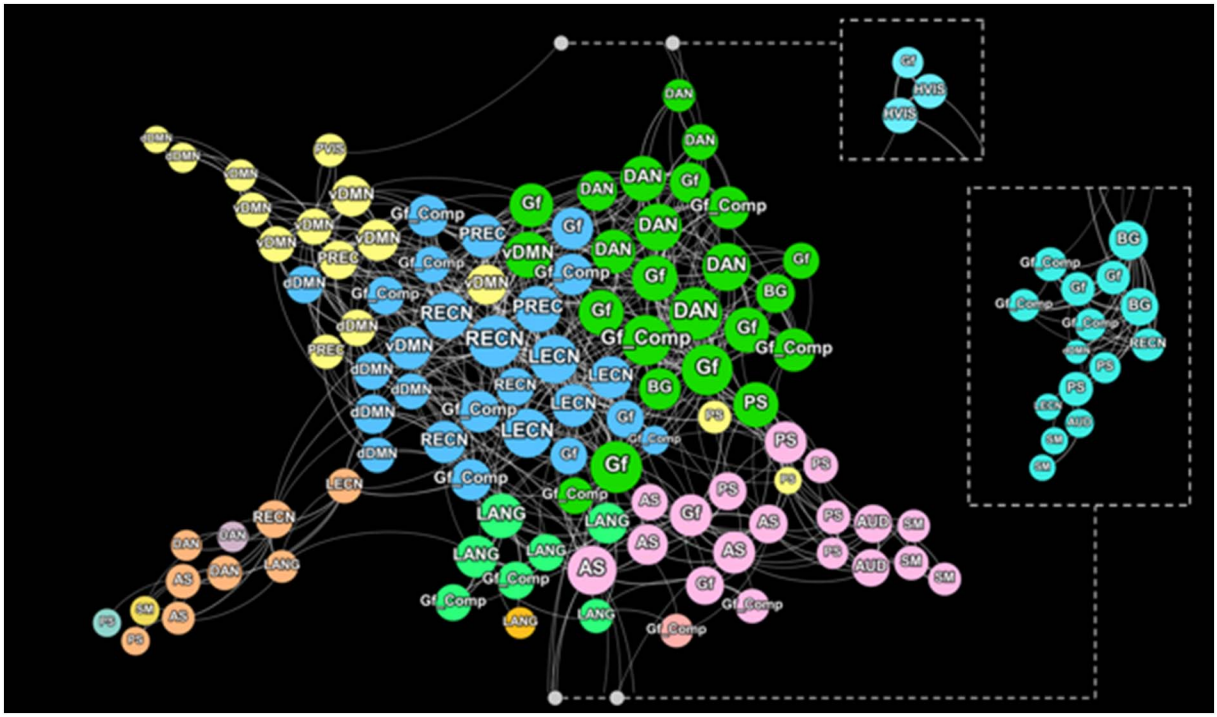

Fig. 6. Modularity analysis. Nodes of the ALE maps representing overall *gf* activation (see Fig. 1) as well as activation clusters for higher complexity trials (*gf*_Comp in the present graph), also see Fig. 2 in (Santarnecchi et al., 2017) are shown as part of a graph also including 90 regions of interest representing nodes of 14 resting-state networks as described in Shirer et al. (2012). Nodal spatial proximity captures the modular structure of resting-state fMRI data, with *gf* regions primarily associated with regions of the DAN, followed by the AS and LECN. Node size represents their nodal degree value. Connections are expressed as binary links with no information about connection strength. For visualization purposes, dotted-line boxes zoom in on segregated section of the graphs. Note: dorsal and ventral default mode networks (vDMN, dDMN); right and left executive control networks (RECN, LECN); dorsal attention network (DAN), anterior and posterior salience networks (AS, PS), basal ganglia network (BG); language network (LANG); high and primary visual networks (HVIS, PVIS); precuneus network (PREC); auditory network (AUD); somatosensory network (SM).

useful for the definition of closed-loop brain stimulation interventions (Lustenberger et al., 2016), with increasing stimulation delivered over the right prefrontal lobe according to trial difficulty. The similarity between the *gf* network and the basal ganglia network is not entirely surprising (Wartenburger, Heekeren, Preusse, Kramer, & van der Meer, 2009), considering previous studies documenting, for instance, a link between intelligence and the caudate nuclei (Rhein et al., 2014), (Melrose, Poulin, & Stern, 2007) and structures of the ventral and dorsal striatum (e.g. caudate nucleus, putamen, and nucleus accumbens) (Schlagenhauf et al., 2013), (Burgaleta et al., 2014). Evidence for the contribution of subcortical structures to high order cognition is not limited to intelligence (Cools, Gibbs, Miyakawa, Jagust, & D'Esposito, 2008; Landau, Lal, O'Neil, Baker, & Jagust, 2009), (Li, Yan, Sinha, & Lee, 2008), (Moffat, Kennedy, Rodrigue, & Raz, 2007), suggesting a need for models taking thalamo-cortical interactions into account.

4.2. Fluid intelligence and the default mode network

A mirrored pattern of connectivity is visible for a core RSN, i.e. the default mode network (DMN). A negative correlation between "task-positive networks" and the DMN has been proposed as a core feature of spontaneous human brain functioning (Fox et al., 2005) and cognitive performance (Spreng, Stevens, Chamberlain, Gilmore, & Schacter, 2010). Interestingly, the intensity of the negative correlation between *gf* and DMN seems even higher than DAN and left/right ECN (Fig. 5B), which are thought as the most negatively correlated networks with the DMN (Fox et al., 2005). This might suggest the correlation between *gf* and DMN as a core feature characterizing *gf* network dynamics at rest. Indeed, the behavioral regression analysis identified a significant link between the *gf* network and multiple functional clusters resembling nodes of the DMN in both the SHARP and Siena datasets, with a strong overlap in the infero-medial prefrontal component of the DMN.

Changes in the strength of the negative correlation between DMN and task-positive networks (e.g. DAN, ASN, FPCN) have been documented in both healthy and pathological aging. Attenuation of the negative correlation between DMN and DAN has been shown in healthy aging participants for both spontaneous and task-related dynamics (Spreng, Stevens, Viviano, & Schacter, 2016). Zhou et al. have documented disease-specific changes in the interplay between the DMN and the anterior salience network (ASN) while comparing patients with frontotemporal dementia (FTD) and Alzheimer's disease (AD) with healthy controls: the magnitude of significantly increase (in FTD) or decrease (in AD) in negative correlation was related to the severity of patients' cognitive decline (Zhou et al., 2010). This evidence suggests that the correlation between DMN and the rest of the brain may represent a pivotal feature of optimal cognitive functioning. At the same time, aging-related decline in *gf* is a characteristic of human cognition, with a constant decrease in performance progressing from around 20 years of age (Salthouse, 2009). Our finding might reconcile the two scenarios, as well as offer some insight on the cognitive reserve model by Stern (2012), suggesting the negative correlation between the DMN and the *gf* network as one of the possible mechanisms behind the aging-related *gf* trajectory as well as the generalized cognitive decline observed in neurodegenerative disorders.

4.3. Potential for network-based analysis of gf dynamics

The high similarity with fMRI RSNs topographies suggests the opportunity for a shift towards a framework where the interaction of *gf*, RSNs and even regions of other cognitive functions of interest (e.g. executive functions (Miyake et al., 2000; Miyake & Friedman, 2012)) can be tested using neuroimaging data. The idea that selective, reproducible perturbation of the human brain might provide even more

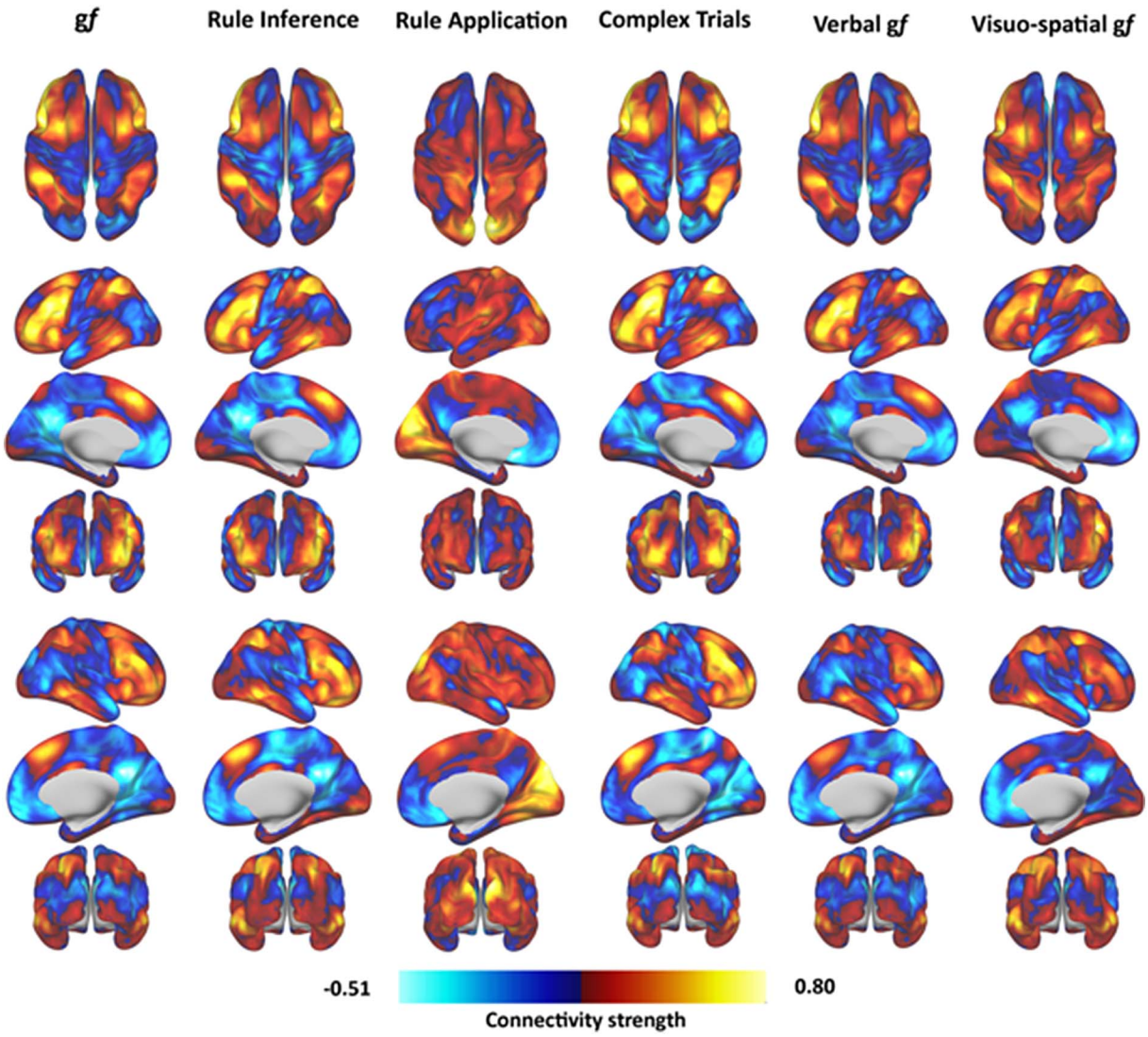

Fig. 7. Functional connectivity of *gf* sub-networks. Seed-based connectivity for *gf* maps describing different processing stages (Rule inference, Rule application), stimuli (verbal, visuo-spatial) and trial complexity are shown. Maps show high similarity, with exception for the Rule application, which mostly loads on regions of the occipital cortex and primary visual network (see also Fig. 3). A difference is also present between verbal and visuo-spatial, with increased involvement of frontal eye fields during processing of visuo-spatial *gf* tasks. Interestingly, solving more complex trial seems to correspond to a greater engagement of regions of the DAN bilaterally, strengthening the association between *gf* and DAN when more complex *gf* processing is required.

information than purely correlational approaches has been promoted in the last two decades (Casali et al., 2013; Massimini, Boly, Casali, Rosanova, & Tononi, 2009), and more recently with a focus on potential applications for intelligence research (Santarnecchi & Rossi, 2016). The field of NIBS is moving towards network-based stimulation approaches (Ruffini, Fox, Ripolles, Miranda, & Pascual-Leone, 2014), suggesting that stimulation of one single node of a network (Santarnecchi et al., 2016), (Santarnecchi et al., 2013), (Pahor & Jausovec, 2014) may be a reductive argument over the complexity of the human brain. The possibility of identifying network-level markers of *gf* abilities must become a priority in order to increase knowledge of the neurobiological underpinnings of human intelligence, as some recent advances in this direction have documented for the general intelligence factor *g* (Hearne et al., 2016). Transcranial electrical and magnetic stimulation approaches could be used to manipulate the negative correlation between *gf* and prefrontal nodes of the DMN, with potential applications in both healthy aging and neurodegenerative conditions.

5. Conclusion

The spontaneous organization of the evoked *gf* network confirms its similarity with fronto-parietal regions of the human brain, suggesting a tighter link to resting-state networks related to attention and cognitive control. Results put forward the negative correlation with the default mode network as a marker of individual differences in *gf* performance, suggesting that the interaction between networks represents the neurophysiological underpinnings of *gf* as well as the target for investigations aimed at its causal manipulation.

Supplementary data to this article can be found online at https://doi.org/10.1016/j.intell.2017.10.002.

Financial disclosures

All authors report no conflict of interest.

Acknowledgement

This research is based upon work supported by the Office of the

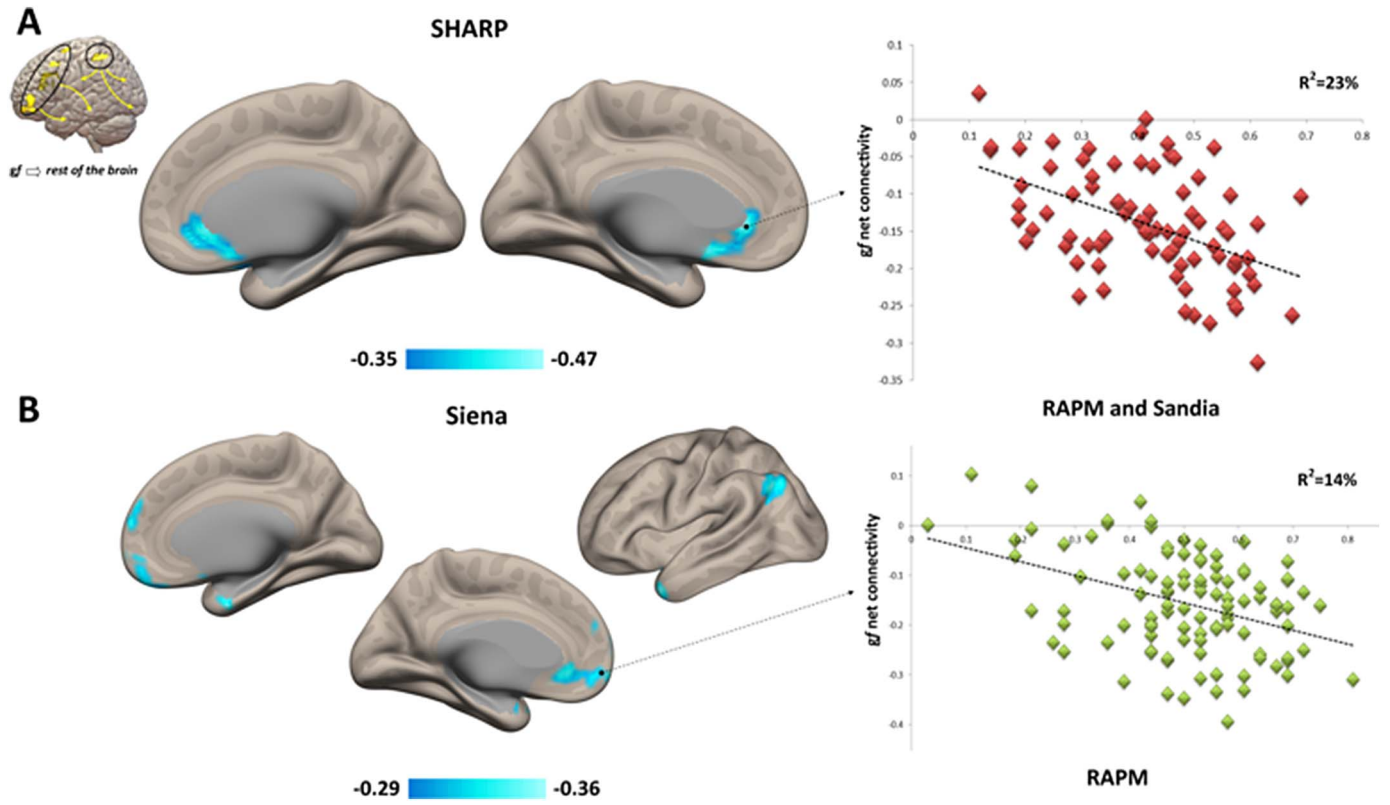

Fig. 8. Behavioral correlates. Results of the regression models built on the (A) SHARP and (B) Siena datasets. Significant clusters ($p < 0.05$ FDR corrected) are displayed in blue-cyan. Scatterplots report correlation between the strength of individual seed-based *gf*-network connectivity and *gf* scores (*x* axis, accuracy values), specifically for the infero-medial prefrontal lobe cluster overlapping in both datasets. Note: RAPM = Raven Advanced Progressive Matrices. (For interpretation of the references to colour in this figure legend, the reader is referred to the web version of this article.)

Director of National Intelligence (ODNI), Intelligence Advanced Research Projects Activity (IARPA), via 2014-13121700007. The views and conclusions contained herein are those of the authors and should not be interpreted as necessarily representing the official policies or endorsements, either expressed or implied, of the ODNI, IARPA, or the U.S. Government. The U.S. Government is authorized to reproduce and distribute reprints for Governmental purposes notwithstanding any copyright annotation thereon. Dr. Pascual-Leone is further supported by the Berenson-Allen Foundation, the Sidney R. Baer Jr. Foundation, grants from the National Institutes of Health (R01HD069776, R01NS073601, R21 MH099196, R21 NS082870, R21 NS085491, R21 HD07616), and Harvard Catalyst. The Harvard Clinical and Translational Science Center (NCRR and the NCATS NIH, UL1 RR025758). The content of this paper is solely the responsibility of the authors and does not necessarily represent the official views of Harvard Catalyst, Harvard University and its affiliated academic health care centers, the National Institutes of Health, the Sidney R. Baer Jr. Foundation. The authors would like to thank the members of the larger Honeywell SHARP team for their valuable contributions to this work, including the SHARP Team authors:

Harvard Medical School (Ann Connor, Franziska Plessow, Sadhvi Saxena, Erica Levenbaum); Honeywell (Jessamy Almquist, Michael Dillard, Umut Orhan, Santosh Mathan); Northeastern University (James McKanna, Deniz Erdogmus, Misha Pavel); Oxford University (Anna-Katharine Brem, Roi Cohen Kadosh, Nick Yeung); SimCoach Games (Garrett Kimball, Eben Myers).

References

Achard, S., & Bullmore, E. (2007). Efficiency and cost of economical brain functional networks. *PLoS Computational Biology, 3*(2), e17. http://dx.doi.org/10.1371/journal.pcbi.0030017.

Adelstein, J. S., Shehzad, Z., Mennes, M., Deyoung, C. G., Zuo, X. N., Kelly, C., ... Milham, M. P. (2011). Personality is reflected in the brain's intrinsic functional architecture. *PLoS One, 6*(11), e27633. http://dx.doi.org/10.1371/journal.pone.0027633.

Agosta, F., Pievani, M., Geroldi, C., Copetti, M., Frisoni, G. B., & Filippi, M. (2012). Resting state fMRI in Alzheimer's disease: Beyond the default mode network. *Neurobiology of Aging, 33*(8), 1564–1578. http://dx.doi.org/10.1016/j.neurobiolaging.2011.06.007.

Allen, E. A., Damaraju, E., Plis, S. M., Erhardt, E. B., Eichele, T., & Calhoun, V. D. (2014). Tracking whole-brain connectivity dynamics in the resting state. *Cerebral Cortex, 24*(3), 663–676. http://dx.doi.org/10.1093/cercor/bhs352.

Anguera, J. A., & Gazzaley, A. (2015). Video games, cognitive exercises, and the enhancement of cognitive abilities. *Current Opinion in Behavioral Sciences, 4*, 160–165. http://dx.doi.org/10.1016/j.cobeha.2015.06.002.

Bassett, D. S., Bullmore, E., Verchinski, B. A., Mattay, V. S., Weinberger, D. R., & Meyer-Lindenberg, A. (2008). Hierarchical organization of human cortical networks in health and schizophrenia. *The Journal of Neuroscience, 28*(37), 9239–9248. http://dx.doi.org/10.1523/JNEUROSCI.1929-08.2008.

Biswal, B. B., Mennes, M., Zuo, X. N., Gohel, S., Kelly, C., Smith, S. M., ... Milham, M. P. (2010). Toward discovery science of human brain function. *Proceedings of the National Academy of Sciences of the United States of America, 107*(10), 4734–4739. http://dx.doi.org/10.1073/pnas.0911855107.

Bonavita, S., Sacco, R., Esposito, S., d'Ambrosio, A., Della, C. M., Corbo, D., ... Tedeschi, G. (2016). Default mode network changes in multiple sclerosis: A link between depression and cognitive impairment? *European Journal of Neurology*. 1468–1331 (Electronic) https://doi.org/10.1111/ene.13112.

Botvinick, M., Nystrom, L. E., Fissell, K., Carter, C. S., & Cohen, J. D. (1999). Conflict monitoring versus selection-for-action in anterior cingulate cortex. *Nature, 402*(6758), 179–181. http://dx.doi.org/10.1038/46035.

Botvinick, M. M., Braver, T. S., Barch, D. M., Carter, C. S., & Cohen, J. D. (2001). Conflict monitoring and cognitive control. *Psychological Review, 108*(3), 624–652.

Botvinick, M. M., Cohen, J. D., & Carter, C. S. (2004). Conflict monitoring and anterior cingulate cortex: An update. *Trends in Cognitive Sciences, 8*(12), 539–546. http://dx.doi.org/10.1016/j.tics.2004.10.003.

Braun, U., Plichta, M. M., Esslinger, C., Sauer, C., Haddad, L., Grimm, O., ... Meyer-Lindenberg, A. (2012). Test–retest reliability of resting-state connectivity network characteristics using fMRI and graph theoretical measures. *NeuroImage, 59*(2), 1404–1412. http://dx.doi.org/10.1016/j.neuroimage.2011.08.044.

Braver, T. S., & Barch, D. M. (2006). Extracting core components of cognitive control. *Trends in Cognitive Sciences, 10*(12), 529–532. http://dx.doi.org/10.1016/j.tics.2006.10.006.

Bullmore, E., & Sporns, O. (2012). The economy of brain network organization. *Nature Reviews. Neuroscience, 13*(5), 336–349. http://dx.doi.org/10.1038/nrn3214.

Bundesen, C. (1990). A theory of visual attention. *Psychological Review, 97*(4), 523–547.
Bunge, S. A., Wallis, J. D., Parker, A., Brass, M., Crone, E. A., Hoshi, E., & Sakai, K. (2005). Neural circuitry underlying rule use in humans and nonhuman primates. *The Journal of Neuroscience, 25*(45), 10347–10350. http://dx.doi.org/10.1523/JNEUROSCI.2937-05.2005.
Burgaleta, M., MacDonald, P. A., Martinez, K., Roman, F. J., Alvarez-Linera, J., Ramos, G. A., ... Colom, R. (2014). Subcortical regional morphology correlates with fluid and spatial intelligence. *Human Brain Mapping, 35*(5), 1957–1968. http://dx.doi.org/10.1002/hbm.22305.
Carter, C. S., Braver, T. S., Barch, D. M., Botvinick, M. M., Noll, D., & Cohen, J. D. (1998). Anterior cingulate cortex, error detection, and the online monitoring of performance. *Science, 280*(5364), 747–749.
Casali, A. G., Gosseries, O., Rosanova, M., Boly, M., Sarasso, S., Casali, K. R., ... Massimini, M. (2013). A theoretically based index of consciousness independent of esensory processing and behavior. *Science Translational Medicine, 5*(198), 198ra105. http://dx.doi.org/10.1126/scitranslmed.3006294.
Cattell, R. B. (1963). Theory of fluid and crystallized intelligence: A critical experiment. *Journal of Education & Psychology, 54*(1), http://dx.doi.org/10.1016/j.neuroimage.2010.06.016.
Choe, A. S., Jones, C. K., Joel, S. E., Muschelli, J., Belegu, V., Caffo, B. S., ... Pekar, J. J. (2015). Reproducibility and temporal structure in weekly resting-state fMRI over a period of 3.5 years. *PLoS ONE, 10*(10), e0140134. http://dx.doi.org/10.1371/journal.pone.0140134.
Cole, M. W., Yarkoni, T., Repovs, G., Anticevic, A., & Braver, T. S. (2012). Global connectivity of prefrontal cortex predicts cognitive control and intelligence. *The Journal of Neuroscience, 32*(26), 8988–8999. http://dx.doi.org/10.1523/JNEUROSCI.0536-12.2012.
Colom, R., Burgaleta, M., Roman, F. J., Karama, S., Alvarez-Linera, J., Abad, F. J., ... Haier, R. J. (2013). Neuroanatomic overlap between intelligence and cognitive factors: Morphometry methods provide support for the key role of the frontal lobes. *Neuroimage, 72C*, 143–152. 1095–9572 (Electronic) https://doi.org/10.1016/j.neuroimage.2013.01.032.
Colom, R., Chuderski, A., & Santarnecchi, E. (2016). Bridge over troubled water: Commenting on Kovacs and Conway's process overlap theory. *Psychological Inquiry, 27*(3), 181–189. http://dx.doi.org/10.1080/1047840X.2016.1181513.
Colom, R., Haier, R. J., Head, K., Alvarez-Linera, J., Quiroga, M. A., Shih, P. C., & Jung, R. E. (2009). Gray matter correlates offluid, crystallized, and spatial intelligence: Testing the P-FIT model. *Intelligence, 37*(4), 124–135.
Cools, R., Gibbs, S. E., Miyakawa, A., Jagust, W., & D'Esposito, M. (2008). Working memory capacity predicts dopamine synthesis capacity in the human striatum. *The Journal of Neuroscience, 28*(5), 1208–1212. http://dx.doi.org/10.1523/JNEUROSCI.4475-07.2008.
Corbetta, M., Patel, G., & Shulman, G. L. (2008). The reorienting system of the human brain: From environment to theory of mind. *Neuron, 58*(3), 306–324. http://dx.doi.org/10.1016/j.neuron.2008.04.017.
Crottaz-Herbette, S., & Menon, V. (2006). Where and when the anterior cingulate cortex modulates attentional response: Combined fMRI and ERP evidence. *Journal of Cognitive Neuroscience, 18*(5), 766–780. http://dx.doi.org/10.1162/jocn.2006.18.5.766.
Deary, I. (2008). Why do intelligent people live longer? *Nature, 456*(7219), 175–176. http://dx.doi.org/10.1038/456175a.
Desimone, R., & Duncan, J. (1995). Neural mechanisms of selective visual attention. *Annual Review of Neuroscience, 18*, 193–222. 0147–006X (Print) https://doi.org/10.1146/annurev.ne.18.030195.001205.
Dice, L. R. (1945). Measures of the amount of ecologic association between species. *Ecology, 26*(3), 297–302. http://dx.doi.org/10.2307/1932409.
Dosenbach, N. U., Fair, D. A., Cohen, A. L., Schlaggar, B. L., & Petersen, S. E. (2008). A dual-networks architecture of top-down control. *Trends in Cognitive Sciences, 12*(3), 99–105. http://dx.doi.org/10.1016/j.tics.2008.01.001.
Dosenbach, N. U., Fair, D. A., Miezin, F. M., Cohen, A. L., Wenger, K. K., Dosenbach, R. A., ... Petersen, S. E. (2007). Distinct brain networks for adaptive and stable task control in humans. *Proceedings of the National Academy of Sciences of the United States of America, 104*(26), 11073–11078. http://dx.doi.org/10.1073/pnas.0704320104.
Dosenbach, N. U., Visscher, K. M., Palmer, E. D., Miezin, F. M., Wenger, K. K., Kang, H. C., ... Petersen, S. E. (2006). A core system for the implementation of task sets. *Neuron, 50*(5), 799–812. http://dx.doi.org/10.1016/j.neuron.2006.04.031.
Ebisch, S. J., Perrucci, M. G., Mercuri, P., Romanelli, R., Mantini, D., Romani, G. L., ... Saggino, A. (2012). Common and unique neuro-functional basis of induction, visualization, and spatial relationships as cognitive components of fluid intelligence. *NeuroImage, 62*(1), 331–342. http://dx.doi.org/10.1016/j.neuroimage.2012.04.053.
Eguiluz, V. M., Chialvo, D. R., Cecchi, G. A., Baliki, M., & Apkarian, A. V. (2005). Scale-free brain functional networks. *Physical Review Letters, 94*(1), 18102.
Etkin, A., Egner, T., Peraza, D. M., Kandel, E. R., & Hirsch, J. (2006). Resolving emotional conflict: A role for the rostral anterior cingulate cortex in modulating activity in the amygdala. *Neuron, 51*(6), 871–882. http://dx.doi.org/10.1016/j.neuron.2006.07.029.
Expert, P., Evans, T. S., Blondel, V. D., & Lambiotte, R. (2011). Uncovering space-independent communities in spatial networks. *Proceedings of the National Academy of Sciences of the United States of America, 108*(19), 7663–7668. http://dx.doi.org/10.1073/pnas.1018962108.
Filmer, H. L., Dux, P. E., & Mattingley, J. B. (2014). Applications of transcranial direct current stimulation for understanding brain function. *Trends in Neurosciences, 37*, 742–753. 1878–108X (Electronic) https://doi.org/10.1016/j.tins.2014.08.003.
Finn, E. S., Shen, X., Scheinost, D., Rosenberg, M. D., Huang, J., Chun, M. M., ... Constable, R. T. (2015). Functional connectome fingerprinting: Identifying individuals using patterns of brain connectivity. *Nature Neuroscience, 18*(11), 1664–1671. http://dx.doi.org/10.1038/nn.4135.
Fox, M. D., Snyder, A. Z., Vincent, J. L., Corbetta, M., Van Essen, D. C., & Raichle, M. E. (2005). The human brain is intrinsically organized into dynamic, anticorrelated functional networks. *Proceedings of the National Academy of Sciences of the United States of America, 102*(27), 9673–9678. http://dx.doi.org/10.1073/pnas.0504136102.
Geake, J. G., & Hansen, P. C. (2005). Neural correlates of intelligence as revealed by fMRI of fluid analogies. *NeuroImage, 26*(2), 555–564. http://dx.doi.org/10.1016/j.neuroimage.2005.01.035.
Geake, J. G., & Hansen, P. C. (2010). Functional neural correlates of fluid and crystallized analogizing. *NeuroImage, 49*(4), 3489–3497. http://dx.doi.org/10.1016/j.neuroimage.2009.09.008.
Haier, R. J., Jung, R. E., Yeo, R. A., Head, K., & Alkire, M. T. (2005). The neuroanatomy of general intelligence: Sex matters. *NeuroImage, 25*(1), 320–327. http://dx.doi.org/10.1016/j.neuroimage.2004.11.019.
Haier, R. J., Siegel, B. V., Nuechterlein, K. H., Hazlett, E., Wu, J. C., Paek, J., ... Buchsbaum, M. S. (1988). Cortical glucose metabolic- rate correlates of abstract reasoning and attention studied with positron emission tomography. *Intelligence, 12*, 199–217. 1756–0500 (Electronic) https://doi.org/10.1186/1756-0500-3-206.
Hearne, L. J., Mattingley, J. B., & Cocchi, L. (2016). Functional brain networks related to individual differences in human intelligence at rest. *Scientific Reports, 6*(1), http://dx.doi.org/10.1038/srep32328.
Jung, R. E., & Haier, R. J. (2007). The Parieto-Frontal Integration Theory (P-FIT) of intelligence: Converging neuroimaging evidence. *The Behavioral and Brain Sciences, 30*(2), 135–154. http://dx.doi.org/10.1017/S0140525X07001185.
Landau, S. M., Lal, R., O'Neil, J. P., Baker, S., & Jagust, W. J. (2009). Striatal dopamine and working memory. *Cerebral Cortex, 19*(2), 445–454. http://dx.doi.org/10.1093/cercor/bhn095.
Li, C. S., Yan, P., Sinha, R., & Lee, T. W. (2008). Subcortical processes of motor response inhibition during a stop signal task. *NeuroImage, 41*(4), 1352–1363. http://dx.doi.org/10.1016/j.neuroimage.2008.04.023.
Lustenberger, C., Boyle, M. R., Alagapan, S., Mellin, J. M., Vaughn, B. V., & Fröhlich, F. (2016). Feedback-controlled transcranial alternating current stimulation reveals a functional role of sleep spindles in motor memory consolidation. *Current Biology, 26*(16), 2127–2136. http://dx.doi.org/10.1016/j.cub.2016.06.044.
Massimini, M., Boly, M., Casali, A., Rosanova, M., & Tononi, G. (2009). A perturbational approach for evaluating the brain's capacity for consciousness. *Progress in Brain Research, 177*, 201–214. 1875–7855 (Electronic) https://doi.org/10.1016/S0079-6123(09)17714-2.
Matzen, L. E., Benz, Z. O., Dixon, K. R., Posey, J., Kroger, J. K., & Speed, A. E. (2010). Recreating Raven's: Software for systematically generating large numbers of Raven-like matrix problems with normed properties. *Behavior Research Methods, 42*, 525–541. 1554–3528 (Electronic) https://doi.org/10.3758/BRM.42.2.525.
Melrose, R. J., Poulin, R. M., & Stern, C. E. (2007). An fMRI investigation of the role of the basal ganglia in reasoning. *Brain Research, 1142*, 146–158. 0006–8993 (Print) https://doi.org/10.1016/j.brainres.2007.01.060.
Miyake, A., & Friedman, N. P. (2012). The nature and organization of individual differences in executive functions: Four general conclusions. *Current Directions in Psychological Science, 21*(1), 8–14. http://dx.doi.org/10.1177/0963721411429458.
Miyake, A., Friedman, N. P., Emerson, M. J., Witzki, A. H., Howerter, A., & Wager, T. D. (2000). The unity and diversity of executive functions and their contributions to complex “Frontal Lobe” tasks: A latent variable analysis. *Cognitive Psychology, 41*(1), 49–100. http://dx.doi.org/10.1006/cogp.1999.0734.
Moffat, S. D., Kennedy, K. M., Rodrigue, K. M., & Raz, N. (2007). Extrahippocampal contributions to age differences in human spatial navigation. *Cerebral Cortex, 17*(6), 1274–1282. http://dx.doi.org/10.1093/cercor/bhl036.
Pahor, A., & Jausovec, N. (2014). The effects of theta transcranial alternating current stimulation (tACS) on fluid intelligence. *International Journal of Psychophysiology, 93*(3), 322–331. http://dx.doi.org/10.1016/j.ijpsycho.2014.06.015.
Pahor, A., & Jaušovec, N. (2014). Theta–gamma cross-frequency coupling relates to the level of human intelligence. *Intelligence, 46*, 283–290. http://dx.doi.org/10.1016/j.intell.2014.06.007.
Preusse, F., van der Meer, E., Deshpande, G., Krueger, F., & Wartenburger, I. (2011). Fluid intelligence allows flexible recruitment of the parieto-frontal network in analogical reasoning. *Frontiers in Human Neuroscience, 5*, 22. 1662–5161 (Electronic) https://doi.org/10.3389/fnhum.2011.00022.
Rhein, C., Muhle, C., Richter-Schmidinger, T., Alexopoulos, P., Doerfler, A., & Kornhuber, J. (2014). Neuroanatomical correlates of intelligence in healthy young adults: The role of basal ganglia volume. *PLoS One, 9*(4), e93623. http://dx.doi.org/10.1371/journal.pone.0093623.
Ruffini, G., Fox, M. D., Ripolles, O., Miranda, P. C., & Pascual-Leone, A. (2014). Optimization of multifocal transcranial current stimulation for weighted cortical pattern targeting from realistic modeling of electric fields. *Neuroimage, 89*, 216–225. 1095–9572 (Electronic) https://doi.org/10.1016/j.neuroimage.2013.12.002.
Salthouse, T. A. (2009). When does age-related cognitive decline begin? *Neurobiology of Aging, 30*(4), 507–514. http://dx.doi.org/10.1016/j.neurobiolaging.2008.09.023.
Santarnecchi, E., Brem, A. K., Levenbaum, E., Thompson, T., Kadosh, R. C., & Pascual-Leone, A. (2015). Enhancing cognition using transcranial electrical stimulation. *Current Opinion in Behavioural Sciences,* 171–178. 1879–0445 (Electronic) https://doi.org/10.1016/j.cub.2013.06.022.
Santarnecchi, E., Emmendorfer, A., & Pascual-Leone, A.. Dissecting the parieto-frontal correlates of fluid intelligence: A comprehensive ALE meta-analysis study. (2017). https://doi.org (in press).
Santarnecchi, E., Polizzotto, N. R., Godone, M., Giovannelli, F., Feurra, M., Matzen, L., ... Rossi, S. (2013). Frequency-dependent enhancement of fluid intelligence induced by transcranial oscillatory potentials. *Current Biology, 23*, 1449–1453. 1879–0445

(Electronic) https://doi.org/10.1016/j.cub.2013.06.022.
Santarnecchi, E., & Rossi, S. (2016). Advances in the neuroscience of intelligence: From brain connectivity to brain perturbation. *Spanish Journal of Psychology, 19*, E94. 1988–2904 (Electronic) https://doi.org/10.1017/sjp.2016.89.
Santarnecchi, G. G., Polizzotto, N. R., Rossi, A., & Rossi, S. (2014). Efficiency of weak brain connections support general cognitive functioning. *Human Brain Mapping, 35*(9), 4566–4582. http://dx.doi.org/10.1002/hbm.22495.
Santarnecchi, Muller, T., Rossi, S., Sarkar, A., Polizzotto, N. R., Rossi, A., & Cohen Kadosh, R. (2016). Individual differences and specificity of prefrontal gamma frequency-tACS on fluid intelligence capabilities. *Cortex, 75*, 33–43. http://dx.doi.org/10.1016/j.cortex.2015.11.003.
Santarnecchi, Rossi, S., & Rossi, A. (2015). The smarter, the stronger: Intelligence level correlates with brain resilience to systematic insults. *Cortex, 64*, 293–309. 1973–8102 (Electronic) https://doi.org/10.1016/j.cortex.2014.11.005.
Schlagenhauf, F., Rapp, M. A., Huys, Q. J., Beck, A., Wustenberg, T., Deserno, L., ... Heinz, A. (2013). Ventral striatal prediction error signaling is associated with dopamine synthesis capacity and fluid intelligence. *Human Brain Mapping, 34*(6), 1490–1499. http://dx.doi.org/10.1002/hbm.22000.
Shirer, W. R., Ryali, S., Rykhlevskaia, E., Menon, V., & Greicius, M. D. (2012). Decoding subject-driven cognitive states with whole-brain connectivity patterns. *Cerebral Cortex, 22*(1), 158–165. http://dx.doi.org/10.1093/cercor/bhr099.
Simard, I., Luck, D., Mottron, L., Zeffiro, T. A., & Soulieres, I. (2015). Autistic fluid intelligence: Increased reliance on visual functional connectivity with diminished modulation of coupling by task difficulty. *Neuroimage. Clin, 9*, 467–478. 2213–1582 (Electronic) https://doi.org/10.1016/j.nicl.2015.09.007.
Song, J., Desphande, A. S., Meier, T. B., Tudorascu, D. L., Vergun, S., Nair, V. A., ... Prabhakaran, V. (2012). Age-related differences in test-retest reliability in resting-state brain functional connectivity. *PLoS One, 7*(12), e49847. http://dx.doi.org/10.1371/journal.pone.0049847.
Soulieres, I., Dawson, M., Samson, F., Barbeau, E. B., Sahyoun, C. P., Strangman, G. E., ... Mottron, L. (2009). Enhanced visual processing contributes to matrix reasoning in autism. *Human Brain Mapping, 30*(12), 4082–4107.
Sporns, O. (2013). Network attributes for segregation and integration in the human brain. *Current Opinion in Neurobiology*. 1873–6882 (Electronic) https://doi.org/10.1016/j.conb.2012.11.015.
Spreng, R. N., Stevens, W. D., Chamberlain, J. P., Gilmore, A. W., & Schacter, D. L. (2010). Default network activity, coupled with the frontoparietal control network, supports goal-directed cognition. *NeuroImage, 53*(1), 303–317. http://dx.doi.org/10.1016/j.neuroimage.2010.06.016.
Spreng, R. N., Stevens, W. D., Viviano, J. D., & Schacter, D. L. (2016). Attenuated anticorrelation between the default and dorsal attention networks with aging: Evidence from task and rest. *Neurobiology of Aging, 45*, 149–160. 1558–1497 (Electronic) https://doi.org/10.1016/j.neurobiolaging.2016.05.020.
Stern, Y. (2012). Cognitive reserve in ageing and Alzheimer's disease. *Lancet Neurology, 11*, 1006–1012. 1474–4465 (Electronic) https://doi.org/10.1016/S1474-4422(12)70191-6.
Tavor, I., Parker, J. O., Mars, R. B., Smith, S. M., Behrens, T. E., & Jbabdi, S. (2016). Task-free MRI predicts individual differences in brain activity during task performance. *Science, 352*(6282), 216–220. http://dx.doi.org/10.1126/science.aad8127.
Thatcher, R. W., Palmero-Soler, E., North, D. M., & Biver, C. J. (2016). Intelligence and eeg measures of information flow: Efficiency and homeostatic neuroplasticity. *Scientific Reports, 6*(1), http://dx.doi.org/10.1038/srep38890.
Vakhtin, A. A., Ryman, S. G., Flores, R. A., & Jung, R. E. (2014). Functional brain networks contributing to the parieto-frontal integration theory of intelligence. *NeuroImage, 103*, 349–354. http://dx.doi.org/10.1016/j.neuroimage.2014.09.055.
van den Heuvel, M. P., & Hulshoff Pol, H. E. (2010). Exploring the brain network: A review on resting-state fMRI functional connectivity. *European Neuropsychopharmacology, 20*(8), 519–534. http://dx.doi.org/10.1016/j.euroneuro.2010.03.008.
Wartenburger, I., Heekeren, H. R., Preusse, F., Kramer, J., & van der Meer, E. (2009). Cerebral correlates of analogical processing and their modulation by training. *NeuroImage, 48*(1), 291–302. http://dx.doi.org/10.1016/j.neuroimage.2009.06.025.
Woldorff, M. G., Hazlett, C. J., Fichtenholtz, H. M., Weissman, D. H., Dale, A. M., & Song, A. W. (2004). Functional parcellation of attentional control regions of the brain. *Journal of Cognitive Neuroscience, 16*(1), 149–165. http://dx.doi.org/10.1162/089892904322755638.
Yeo, B. T., Krienen, F. M., Sepulcre, J., Sabuncu, M. R., Lashkari, D., Hollinshead, M., ... Buckner, R. L. (2011). The organization of the human cerebral cortex estimated by intrinsic functional connectivity. *Journal of Neurophysiology, 106*(3), 1125–1165. http://dx.doi.org/10.1152/jn.00338.2011.
Yuan, Z., Qin, W., Wang, D., Jiang, T., Zhang, Y., & Yu, C. (2012). The salience network contributes to an individual's fluid reasoning capacity. *Behavioural Brain Research, 229*(2), 384–390. http://dx.doi.org/10.1016/j.bbr.2012.01.037.
Zalesky, A., Fornito, A., Harding, I. H., Cocchi, L., Yucel, M., Pantelis, C., & Bullmore, E. T. (2010). Whole-brain anatomical networks: Does the choice of nodes matter? *NeuroImage, 50*(3), 970–983. http://dx.doi.org/10.1016/j.neuroimage.2009.12.027.
Zhou, J., Greicius, M. D., Gennatas, E. D., Growdon, M. E., Jang, J. Y., Rabinovici, G. D., ... Seeley, W. W. (2010). Divergent network connectivity changes in behavioural variant frontotemporal dementia and Alzheimer's disease. *Brain, 133*(Pt 5), 1352–1367. http://dx.doi.org/10.1093/brain/awq075.